A Comprehensive Kinetic Model for High-Temperature Free Radical Production of Styrene/Methacrylate/Acrylate Resins

Wei Wang and Robin A. Hutchinson
Dept. of Chemical Engineering, Dupuis Hall, Queen's University, Kingston, Ontario K7L 3N6, Canada

DOI 10.1002/aic.12258
Published online April 27, 2010 in Wiley Online Library (wileyonlinelibrary.com).

n-*Butyl methacrylate*/*styrene*/n-*butyl acrylate (BMA*/*ST*/*BA) high-temperature starved-feed solution semibatch copolymerization and terpolymerization experiments with varying monomer feed composition, final polymer content, monomer feed time, and reaction temperature were carried out. A comprehensive mechanistic terpolymerization model implemented in PREDICI includes methacrylate depropagation, acrylate backbiting, chain scission, and macromonomer propagation, as well as penultimate chain-growth and termination kinetics. The generality of the model was verified by comparison with terpolymerization data sets from two laboratories that demonstrate the impact of high-temperature secondary reactions on polymerization rate and polymer molecular weight*. © 2010 American Institute of Chemical Engineers *AIChE J,* 57: 227–238, 2011

Keywords: terpolymerization, kinetics (polym.), methacrylate, acrylate, styrene, mechanistic model, depropagation, intramolecular transfer to polymer, chain scission, macromonomer reactions, midchain radical

Introduction

Acrylic resins, synthesized from a mixture of monomers selected from the methacrylate, acrylate, and styrene (ST) families, are the base polymer components for many automotive coatings due to their excellent chemical and mechanical properties. The low-molecular weight (MW) polymers, synthesized via high-temperature starved-feed free-radical solution semibatch terpolymerization,[1,2] contain reactive functionalities that serve as crosslinking sites for polymer network formation upon application.[3,4] The operating conditions, chosen to reduce the amount of initiator required in the recipe and to keep solution viscosity low, greatly promote the importance of secondary reactions, such as methacrylate depropagation, acrylate branching, chain β-scission, and macromonomer reactions, that have a strong impact on polymerization rate and polymer MW. Understanding these kinetic complexities is the goal of this effort to develop a generalized model that can be utilized for process development and optimization and to develop new coatings recipes with reduced experimentation.

In radical polymerization, polymer chains grow quickly through the sequential addition of monomer to the radical center (denoted by $P_n^\bullet$) with propagation rate coefficient k_p. At higher temperature conditions, the rate of the reverse reaction, known as depropagation (rate coefficient k_{dp}), becomes appreciable:

$$P_n^\bullet + M \underset{k_{dp}}{\overset{k_p}{\rightleftarrows}} P_{n+1}^\bullet$$

This reaction is thermodynamically controlled and the ratio of the forward to reverse rate constants is given by the equilibrium constant, $K = k_p/k_{dp}$, where $K = [M]_{eq}^{-1}$ and $[M]_{eq}$ is the equilibrium monomer concentration at a given temperature. At a fixed temperature, polymerization will not

Correspondence concerning this article should be addressed to R. A. Hutchinson at robin.hutchinson@chee.queensu.ca.
Current Address of Wei Wang: PPG Industries, Coatings Innovation Center, 4325 Rosanna Drive, Allison Park, PA 15101.

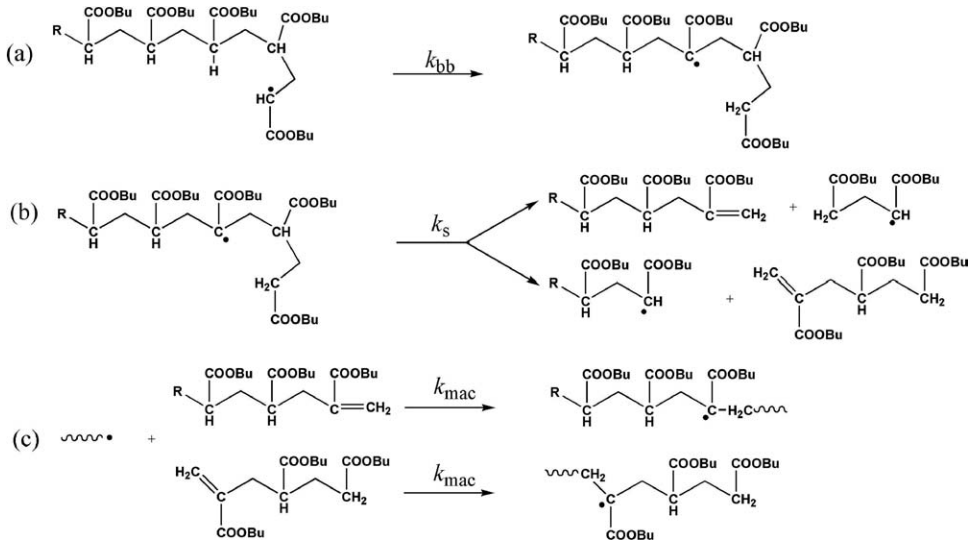

Scheme 1. Acrylate intramolecular chain transfer (a), chain scission (b), and macromonomer addition (c).

proceed if $[M]$ is below $[M]_{eq}$. The mechanism becomes important for homopolymerization of methacrylate monomers at temperatures >120°C, depending on monomer concentration,[5,6] and has a significant effect on polymerization rate under the starved-feed high-temperature conditions used to manufacture acrylic coatings resins.[2,7,8] More recently, high-temperature studies of butyl methacrylate (BMA) semibatch polymerization indicated that depropagation is not only a function of temperature but also of the polymer weight fraction in the reaction system,[2,9] as would be expected from thermodynamic considerations.[10] ST and acrylates do not depropagate at appreciable rates under similar reaction conditions, and thus lessen the impact of this mechanism during copolymerization. Nonetheless, depropagation has an effect on copolymer composition and polymerization rate when methacrylates copolymerize with acrylates[8] and ST[7,11,12] under high-temperature starved-feed conditions. A kinetic investigation of BMA and ST copolymerization showed that the Lowry Case 1 model[13] is adequate to predict depropagation in the binary system, i.e., BMA will only depropagate when another BMA exists in the penultimate position.[14] The modeling of the copolymerization kinetics becomes more involved if the penultimate unit also affects chain-growth kinetics, but these complications have also been addressed.[15]

In free radical polymerization of acrylates, it is now well-accepted that the propagating secondary butyl acrylate (BA) radical can undergo backbiting (intramolecular chain transfer to polymer, Scheme 1a) even at ambient temperature to form midchain radicals that can then subsequently propagate or terminate,[16–19] or, at higher temperatures, form macromonomer via β-scission (Scheme 1b).[20–27] At higher temperatures under starved-feed conditions it was concluded that the majority of the poly(BA) chains in the system had been terminated by β-scission even in the presence of high initiator levels, as demonstrated by significant amounts of macromonomer measured by ^{1}H NMR,[22] and the mechanisms were included in mechanistic models developed to represent acrylate homo-[22,23] and copolymerizations[8] at higher temperatures. However, as shown in Scheme 1b, a product of chain β-scission is a polymer chain with an unsaturated endgroup (i.e., a macromonomer) that, as suggested by Yamada et al.,[21,28,29] may be as reactive as monomer. The importance of macromonomer propagation (Scheme 1c) under high-temperature starved-feed semibatch conditions has recently been demonstrated and modeled, with the macromonomer reaction responsible for the significant increase in polymer weight-average molecular weight (M_w) with time.[30]

The addition of comonomer to an acrylate polymerization complicates the set of mechanisms shown in Scheme 1. The study on BA/BMA copolymerization[8] indicated that backbiting occurs only when an acrylate radical finds an acrylate unit in its pen-penultimate position, and modeled the system assuming that β-scission of the resultant midchain radical occurs 10 times faster with an adjacent methacrylate unit than with an adjacent acrylate unit, due to the higher stability of the resulting tertiary carbon-centered radical. As acrylate backbiting occurs via a six-membered ring transition state, the identity of the penultimate unit may affect the rate of the intramolecular H-atom abstraction through steric effects. Indeed, our recent work on BA/ST copolymerization[31] suggested that the rate of backbiting should be reduced when ST is in the penultimate position, as also suggested by Plessis et al.[32] for ST/BA and González et al.[33] for BA/MMA (methyl methacrylate) copolymerization; the latter two studies used ^{13}C NMR to quantify the amount of acrylate backbiting that occurs during copolymerization.

Mechanistic modeling provides a means to study the effect of secondary reactions (such as depropagation, backbiting, and scission) on copolymerization kinetics and also is a critical component of larger-scale process models used to predict the influence of operating conditions on reaction rate and polymer properties, guide the selection and optimization of standard operating conditions for existing and new polymer grades, and guide process development from laboratory to pilot-plant to full-scale production. The secondary kinetic steps introduce greater complexities to the modeling of multicomponent polymerizations. The terpolymerization models of BA/MMA/VAc (vinyl acetate) developed by Penlidis

et al.[34,35] and Keramopoulos et al.[36] are limited to low temperatures (50 and 70°C) and none of the side reactions discussed above were included. Depropagation is included in the modeling of higher-temperature (115 and 140°C) free radical terpolymerization of BA/MMA/α-methyl ST,[37,38] but the acrylate side reactions were not considered, as the model focused only on terpolymer composition.

In this work, a comprehensive BMA/BA/ST terpolymerization mechanistic model, including the secondary reactions mentioned above, as well as penultimate chain-growth and chain-termination kinetics, is formulated to represent high-temperature solution acrylic terpolymerization. The model was developed and implemented in the commercial software PREDICI,[39] and, via comparison with an extensive set of copolymerization and terpolymerization experiments, is used to demonstrate the importance of secondary reactions on polymerization rate (e.g., monomer concentrations) and polymer MW profiles under starved-feed high-temperature semibatch conditions.

Experimental

Materials

BMA (99% purity) inhibited with 10 ppm of monomethyl ether hydroquinone, ST (99% purity) inhibited with 10–15 ppm of 4-tert-butylcatechol, and BA (99% purity) with 10–55 ppm monomethyl ether hydroquinone as inhibitor were obtained from Sigma Aldrich and used as received. *tert*-butyl peroxyacetate (TBPA) was provided as a solution of 75 wt % initiator in mineral spirits by Arkema, and a xylene isomeric mixture with boiling point range between 136 and 140°C was obtained from Sigma-Aldrich and used as received.

Semibatch solution polymerization

Semibatch solution polymerizations were carried out as described previously.[1] Initiator and monomer feed rates to the 1 l agitated reactor and reactor temperature were automatically controlled. The reactor was charged with xylene solvent and brought up to the desired reaction temperature (e.g., 138°C) under nitrogen blanket. Once at temperature, monomer and initiator solutions were continuously fed at a fixed rate over the complete reaction period, with initiator fed for an extra 15 min to drive the polymerization to completion; the total amounts added were adjusted to achieve the desired polymer content and initiator level for a particular recipe. The experiments are described according to final polymer content (monomer/(monomer + solvent) on a weight basis), mass ratio of the two monomers in the feed, and the amount of initiator added relative to monomer on a weight basis. Samples of approximately 1–2 ml were drawn from the reactor at specified times into ice-cold 4-methoxyphenol (1 g l^{-1}) xylene solution to terminate the reaction.

It should be noted that two different experimental data sets were used. The primary set of data discussed was obtained in our lab, with experiments generally conducted with 70 wt % final polymer content, a monomer feeding time of 6 h, and an initiator level of 2 wt % relative to monomer. Additional data were provided by a DuPont laboratory, with experiments conducted at various temperatures and polymer content using the same experimental procedure, but with a monomer feeding time of 3 h and initiator level of 1.5 mol % relative to monomer.

Characterization of polymer products

The residual monomer concentrations in the samples were determined using a Varian CP-3800 gas chromatograph (GC) setup, as detailed before.[11] Calibration standards were constructed by mixing measured quantities of ST, BMA, and BA monomers into a known mass of acetone, and a linear calibration curve was constructed by plotting peak area vs. monomer concentration. Size-exclusion chromatography (SEC), used to determine the MW of the polymer samples, was performed using a Waters 2960 separation module with a Waters 410 differential refractometer (RI detector) and a Wyatt Technology Light Scattering detector (LS detector). Tetrahydrofuran (THF) was used as the eluent at a flow rate of 1 ml min^{-1}, and Styragel packed columns HR 0.5, HR 1, HR 3, and HR 4 (Waters Division Millipore) were used. Calibration for the RI detector was established using eight linear narrow PDI polystyrene standards over a MW range from 890 to 3.55×10^5 g mol^{-1}, with copolymer MW values calculated by universal calibration using known Mark-Houwink parameters (poly(ST): $K = 1.14 \times 10^{-4}$ ml g^{-1} and $a = 0.716$[40]; poly(BMA): $K = 1.48 \times 10^{-4}$ ml g^{-1} and $a = 0.664$[14]; poly(BA): $K = 1.22 \times 10^{-4}$ ml g^{-1} and $a = 0.70$[41]). The output signal of the LS detector provides the absolute molar mass without the need for calibration standards but with knowledge of the dn/dc values [poly(ST): $dn/dc = 0.180$[14]; poly(BMA): $dn/dc = 0.080$[14]; poly(BA): $dn/dc = 0.070$[41]; all values in ml g^{-1}]. For both detectors, copolymer and terpolymer MWs are calculated as a composition weighted average of the homopolymer values, a methodology verified in previous work.[14,40,42,43] MW averages calculated using the two detectors are within 15%,[11,12] and the weight-average MW values (M_w) reported in this work are from the LS detector. Experiments conducted at identical conditions for this semibatch system show good reproducibility; relative error in monomer concentration profiles typically is within 10%, and MW data are within 15%.[44]

Model Development

The full methacrylate/acrylate/ST terpolymerization mechanistic model is based on our previous methacrylate/acrylate,[8] methacrylate/ST,[1] and ST/acrylate[31] models. It includes all of the secondary reactions discussed in the Introduction, such as methacrylate depropagation, acrylate backbiting, β-scission of midchain radicals, and macromonomer addition, as shown in Table 1. The subscript n (or r) denotes the number of monomeric units in growing chain-end polymer radicals ($P_n^{j\bullet}$ and $P_r^{k\bullet}$), midchain radicals ($Q_n^{\bullet}$ and $Q_r^{\bullet}$), dead polymer chains (D_n and D_r), and macromonomers (U_n), whereas the superscript j or k represents the growing polymer radicals ending with monomer unit j (M_j) or monomer unit k (M_k). ST self-thermal polymerization is neglected due to the high initiator level (2 wt % initiator/monomer) and low-monomer concentration in our system. Inhibition is also not considered in the model because the inhibitor is present at levels less than 0.1% of the initiator. The model is

Table 1. Kinetic Mechanisms of High-Temperature BMA(1)/ST(2)/BA(3) Terpolymerization

Initiation	$I \xrightarrow{k_d} 2fI^{\bullet}$
	$I^{\bullet} + M_j \xrightarrow{k_{p_{1ji}}} P_1^{j\bullet}$
Propagation	$P_n^{j\bullet} + M_k \xrightarrow{P_{ij}k_{p_{ijk}}} P_{n+1}^{k\bullet}$
Chain transfer to solvent	$P_n^{j\bullet} + S \xrightarrow{C_{s,j}k_{p_{1ji}}} S^{\bullet} + D_n$
	$S^{\bullet} + M_j \xrightarrow{k_{p_{1ji}}} P_1^{j\bullet}$
Termination	
By combination	$P_n^{ij\bullet} + P_r^{kl\bullet} \xrightarrow{k_{tc_{ij,kl}}} D_{n+r}$
By disproportionation	$P_n^{ij\bullet} + P_r^{kl\bullet} \xrightarrow{k_{td_{ij,kl}}} D_n + D_r$
Depropagation	$P_{n+1}^{1\bullet} \xrightarrow{P_{11}k_{dp}} P_n^{1\bullet} + M_1$
Intramolecular chain transfer (backbiting)	$P_n^{3\bullet} \xrightarrow{P_{33}P_{33}k_{bb}} Q_{n,SCB}^{333\bullet}$
	$P_n^{3\bullet} \xrightarrow{0.6\times P_{31}P_{13}k_{bb}} Q_{n,SCB}^{313\bullet}$
	$P_n^{3\bullet} \xrightarrow{0.6\times P_{32}P_{23}k_{bb}} Q_{n,SCB}^{323\bullet}$
β-scission	$Q_{n,SCB}^{333\bullet} \xrightarrow{k_s} U_{n-2} + P_2^{3\bullet};$
	$Q_{n,SCB}^{333\bullet} \xrightarrow{P_{23}f_{ST}k_s} P_{n-3}^{2\bullet} + U_3$
	$Q_{n,SCB}^{333\bullet} \xrightarrow{P_{33}k_s} P_{n-3}^{3\bullet} + U_3;$
	$Q_{n,SCB}^{333\bullet} \xrightarrow{P_{13}f_{BMA}k_s} P_{n-3}^{1\bullet} + U_3$
	$Q_{n,SCB}^{313\bullet} \xrightarrow{f_{BMA}k_s} U_{n-2} + P_2^{1\bullet};$
	$Q_{n,SCB}^{313\bullet} \xrightarrow{P_{33}k_s} P_{n-3}^{3\bullet} + U_3$
	$Q_{n,SCB}^{313\bullet} \xrightarrow{P_{13}f_{BMA}k_s} P_{n-3}^{1\bullet} + U_3;$
	$Q_{n,SCB}^{313\bullet} \xrightarrow{P_{23}f_{ST}k_s} P_{n-3}^{2\bullet} + U_3$
	$Q_{n,SCB}^{323\bullet} \xrightarrow{f_{ST}k_s} U_{n-2} + P_2^{2\bullet};$
	$Q_{n,SCB}^{323\bullet} \xrightarrow{P_{33}k_s} P_{n-3}^{3\bullet} + U_3$
	$Q_{n,SCB}^{323\bullet} \xrightarrow{P_{13}f_{BMA}k_s} P_{n-3}^{1\bullet} + U_3;$
	$Q_{n,SCB}^{323\bullet} \xrightarrow{P_{23}f_{ST}k_s} P_{n-3}^{2\bullet} + U_3$
Chain branching*	$Q_n^{\bullet} + M_j \xrightarrow{k_p^t/r_{3j}} P_{n+1}^{j\bullet}$
Termination of tertiary radicals*	
By combination	$Q_n^{\bullet} + Q_r^{\bullet} \xrightarrow{k_{tc,qq}} D_{n+r}$
	$Q_n^{\bullet} + P_r^{j\bullet} \xrightarrow{k_{tc,pq}} D_{n+r}$
By disproportionation	$Q_n^{\bullet} + Q_r^{\bullet} \xrightarrow{k_{td,qq}} D_n + D_r$
	$Q_n^{\bullet} + P_r^{j\bullet} \xrightarrow{k_{td,pq}} D_n + D_r$
Long-chain branching†	$P_n^{j\bullet} + D_r \xrightarrow{k_{tr,pol}\times F_3\times\frac{k_{pjij}}{k_{p333}}\times r} D_n + Q_{r,LCB}^{\bullet}$
	$I^{\bullet} + D_r \xrightarrow{k_{tr,pol}^{I\bullet}\times F_3\times r} Q_{r,LCB}^{\bullet}$
Macromonomer propagation	$P_n^{1\bullet} + U_r \xrightarrow{0.55\times k_{p111}} Q_{n+r,LCB}^{\bullet}$
	$P_n^{2\bullet} + U_r \xrightarrow{0.55\times k_{p222}/r_{21}} Q_{n+r,LCB}^{\bullet}$
	$P_n^{3\bullet} + U_r \xrightarrow{0.55\times k_{p333}} Q_{n+r,LCB}^{\bullet}$

*These reactions occur for both $Q_{SCB}^{\bullet}$ and $Q_{LCB}^{\bullet}$.
†F_3 represents the BA mole fraction in the polymer chain; long-chain branching reactions involving macromonomer (U_r instead of D_r) are also allowed to occur.

implemented in the commercial software PREDICI,[39] with all the rate coefficients listed in Table 2 obtained from literature and previous work.

By considering the penultimate unit of the radicals, there are 27 propagation reactions for terpolymerization (see Scheme 2). $k_{P_{ijk}}$ represents the monomer addition rate coefficient of monomer k to radical ij, and k_{dp} represents the depropagation rate coefficient of the BMA radical. P_{ij} is the fraction of radical j with i unit present in the penultimate position, introduced in order to define the product radical formed when depropagation occurs. Thus,

$$P_{11} = \frac{P^{11\bullet}}{P^{11\bullet} + P^{21\bullet} + P^{31\bullet}} \qquad P_{22} = \frac{P^{22\bullet}}{P^{32\bullet} + P^{22\bullet} + P^{12\bullet}}$$

$$P_{33} = \frac{P^{33\bullet}}{P^{13\bullet} + P^{23\bullet} + P^{33\bullet}} \quad (1)$$

where $P^{ij\bullet}$ represents all radicals ending in ij, $P^{ij\bullet} = \sum_{n=1}^{\infty} P_n^{ij\bullet}$. From these definitions it is clear that $P_{11} + P_{21} + P_{31} = 1$, $P_{12} + P_{22} + P_{31} = 1$, and $P_{13} + P_{23} + P_{33} = 1$.

To implement the propagation and depropagation steps in the terpolymerization model, these probabilities were solved and expressed as functions of monomer fractions and rate coefficients. This was done by performing balances on radical species $P^{11\bullet}$ (Eq. 2), $P^{22\bullet}$ (Eq. 3), $P^{33\bullet}$ (Eq. 4), $P^{32\bullet}$ (Eq. 5), $P^{23\bullet}$ (Eq. 6), $P^{12\bullet}$ (Eq. 7), $P^{21\bullet}$ (Eq. 8), $P^{13\bullet}$ (Eq. 9), and $P^{31\bullet}$ (Eq. 10) under the long-chain hypothesis and assuming radical stationarity, and applying the definitions of probabilities:

$$P_{11}k_{p_{113}}[M_3] + P_{11}k_{p_{112}}[M_2] + (P_{21} + P_{31})P_{11}k_{dep} - P_{31}k_{p_{311}}[M_1] - P_{21}k_{p_{211}}[M_1] = 0 \quad (2)$$

$$P_{22}k_{p_{223}}[M_3] + P_{22}k_{p_{221}}[M_1] - P_{32}k_{p_{322}}[M_2] - P_{12}k_{p_{122}}[M_2] = 0 \quad (3)$$

$$P_{33}k_{p_{331}}[M_1] + P_{33}k_{p_{332}}[M_2] - P_{13}k_{p_{133}}[M_3] - P_{23}k_{p_{233}}[M_3] = 0 \quad (4)$$

$$\left[P^{2\bullet}\right] = \left(\frac{P_{33}k_{p_{332}}[M_2] + P_{13}k_{p_{132}}[M_2] + P_{23}k_{p_{232}}[M_2]}{P_{32}k_{p_{323}}[M_3] + P_{32}k_{p_{321}}[M_1] + P_{32}k_{p_{322}}[M_2]}\right)\left[P^{3\bullet}\right] \quad (5)$$

$$P_{23}k_{p_{233}}\left[P^{3\bullet}\right][M_3] + P_{23}k_{p_{231}}\left[P^{3\bullet}\right][M_1] + P_{23}k_{p_{232}}\left[P^{3\bullet}\right][M_2] = P_{22}k_{p_{223}}\left[P^{2\bullet}\right][M_3] + P_{32}k_{p_{323}}\left[P^{2\bullet}\right][M_3] + P_{12}k_{p_{123}}\left[P^{2\bullet}\right][M_3] \quad (6)$$

$$\left[P^{2\bullet}\right] = \left(\frac{P_{11}k_{p_{112}}[M_2] + P_{31}k_{p_{312}}[M_2] + P_{21}k_{p_{212}}[M_2]}{P_{12}k_{p_{123}}[M_3] + P_{12}k_{p_{121}}[M_1] + P_{12}k_{p_{122}}[M_2]}\right)\left[P^{1\bullet}\right] \quad (7)$$

$$P_{21}k_{p_{213}}\left[P^{1\bullet}\right][M_3] + P_{21}k_{p_{211}}\left[P^{1\bullet}\right][M_1] + P_{21}k_{p_{212}}\left[P^{1\bullet}\right][M_2] - P_{21}P_{11}k_{dep}\left[P^{1\bullet}\right] = P_{22}k_{p_{221}}\left[P^{2\bullet}\right][M_1] + P_{32}k_{p_{321}}\left[P^{2\bullet}\right][M_1] + P_{12}k_{p_{121}}\left[P^{2\bullet}\right][M_1] \quad (8)$$

$$\left[P^{3\bullet}\right] = \left(\frac{P_{11}k_{p113}[M_3] + P_{31}k_{p313}[M_3] + P_{21}k_{p_{213}}[M_3]}{P_{13}k_{p_{133}}[M_3] + P_{13}k_{p_{131}}[M_1] + P_{13}k_{p_{132}}[M_2]}\right)\left[P^{1\bullet}\right] \quad (9)$$

Table 2. Model Rate Coefficients and Parameters (1 = BMA; 2 = ST; and 3 = BA)

	Rate Expression	Reference
Initiation	$k_d(s^{-1}) = 6.78 \times 10^{15} \exp(-17714/T); f = 0.50$	45
Propagation	$k_{p_{111}}\left(L \cdot mol^{-1} \cdot s^{-1}\right) = 3.80 \times 10^6 \exp(-2754.2/T)$	46
	$k_{p_{222}}\left(L \cdot mol^{-1} \cdot s^{-1}\right) = 4.266 \times 10^7 \exp(-3910/T)$	47
	$k_{p_{333}}\left(L \cdot mol^{-1} \cdot s^{-1}\right) = 1.8 \times 10^7 \exp(-2074/T)$	48
	$r_{13} = 0.8268 \exp(282.1/T); r_{31} = 1.5815 \exp(-564.8/T)$	49
	$r_{12} = 0.42; r_{21} = 0.61; r_{23} = 0.877; r_{32} = 0.241$	50
	$s_{13} = 0.43; s_{31} = 1.98; s_{23} = 0.11; s_{32} = 0.9; s_{12} = 0.44; s_{21} = 0.62$	50
Termination	$k_{t_{11}}\left(L \cdot mol^{-1} \cdot s^{-1}\right) = 1.1 \times 10^9 \exp(-1241/T)$	51
	$k_{t_{22}}\left(L \cdot mol^{-1} \cdot s^{-1}\right) = 3.18 \times 10^9 \exp(-958/T)$	52
	$k_{t_{33}}\left(L \cdot mol^{-1} \cdot s^{-1}\right) = 3.89 \times 10^9 \exp(-1010/T)$	53
	$k_{t,ter}^{0.5} = (k_{t_{11}}^{0.5} P^{11\bullet} + k_{t_{12,12}}^{0.5} P^{12\bullet} + k_{t_{13,13}}^{0.5} P^{13\bullet} + k_{t_{22}}^{0.5} P^{22\bullet} + k_{t_{21,21}}^{0.5} P^{21\bullet} + k_{t_{23,23}}^{0.5} P^{23\bullet} + k_{t_{33}}^{0.5} P^{33\bullet} + k_{t_{31,31}}^{0.5} P^{31\bullet} + k_{t_{32,32}}^{0.5} P^{32\bullet})/(P^{1\bullet} + P^{2\bullet} + P^{3\bullet})$	1
	$k_{tij,ij} = (k_{tii} \times k_{tij})^{0.5}$	
	$k_{td_{11}}/k_{t,terpo} = 0.65; \quad k_{td_{33}}/k_{t,terpo} = 0.05$	1,31
	$k_{td_{22}}/k_{t,terpo} = 0.01; \quad k_{td_{12}}/k_{t,terpo} = 0.33$	
	$k_{td_{13}}/k_{t,terpo} = 0.35; \quad k_{td_{23}}/k_{t,terpo} = 0.03$	
Transfer to solvent	$C_{s,1} = 25 \exp(-4590/T)$	9
	$C_{s,2} = 56 \exp(-4590/T)$	1
	$C_{s,3} = 96 \exp(-4443/T)$	30,54
Depropagation	$[M]_{eq} = \frac{k_{dp}}{k_{p_{111}}} = \left(1.76 \times 10^6 - 1.37 \times 10^6 x_{wp}\right) \exp(-6240/T)$	9
Backbiting	$k_{bb}(s^{-1}) = 7.41 \times 10^7 \exp(-3933/T)$	54
Scission	$k_s(s^{-1}) = 3.3 \times 10^9 \exp(-7989/T)$	30
	$f_{ST} = 50; f_{BMA} = 10$	8,31
Chain branching	$k_p^t = 1.2 \times 10^6 \exp(-3440/T)$	54
Termination of tertiary radicals	$k_{t,qq} = 5.3 \times 10^9 \exp(-2357/T)$	53
	$k_{t,pq} = (k_{t,qq} \times k_{t,terpo})^{0.5}$	
Long chain branching	$k_{tr,pol}/k_{p_{333}} = 1 \times 10^{-4}$	30
	$k_{tr,pol}^{I\bullet}/k_{p333} = 0.01$	30

$$P_{31}k_{p_{313}}\left[P^{1\bullet}\right][M_3] + P_{31}k_{p_{311}}\left[P^{1\bullet}\right][M_1] + P_{31}k_{p_{312}}\left[P^{1\bullet}\right][M_2] = P_{33}k_{p_{331}}\left[P^{3\bullet}\right][M_1] + P_{13}k_{p_{131}}\left[P^{3\bullet}\right][M_1] + P_{23}k_{p_{231}}\left[P^{3\bullet}\right][M_1] + P_{31}P_{11}k_{dep}\left[P^{1\bullet}\right] \quad (10)$$

Adding Eqs 5–6, Eqs 7–8 and making some rearrangements, the following set of equations can be obtained:

$$\left(P_{22}k_{p_{223}}[M_3] + P_{32}k_{p_{323}}[M_3] + P_{12}k_{p_{123}}[M_3]\right)\bullet Y - \left(P_{23}k_{p_{233}}[M_3] + P_{23}k_{p_{231}}[M_1] + P_{23}k_{p_{232}}[M_2]\right) = 0 \quad (11)$$

$$\begin{array}{lll}
P_n^{11\bullet} + M_1 \underset{P_{11}k_{dp}}{\overset{k_{p111}}{\rightleftharpoons}} P_{n+1}^{11\bullet} & P_n^{11\bullet} + M_2 \xrightarrow{k_{p112}} P_{n+1}^{12\bullet} & P_n^{11\bullet} + M_3 \xrightarrow{k_{p113}} P_{n+1}^{13\bullet} \\
P_n^{12\bullet} + M_1 \xrightarrow{k_{p121}} P_{n+1}^{21\bullet} & P_n^{12\bullet} + M_2 \xrightarrow{k_{p122}} P_{n+1}^{22\bullet} & P_n^{12\bullet} + M_3 \xrightarrow{k_{p123}} P_{n+1}^{23\bullet} \\
P_n^{13\bullet} + M_1 \xrightarrow{k_{p131}} P_{n+1}^{31\bullet} & P_n^{13\bullet} + M_2 \xrightarrow{k_{p132}} P_{n+1}^{32\bullet} & P_n^{13\bullet} + M_3 \xrightarrow{k_{p133}} P_{n+1}^{33\bullet} \\
P_n^{22\bullet} + M_1 \xrightarrow{k_{p221}} P_{n+1}^{21\bullet} & P_n^{22\bullet} + M_2 \xrightarrow{k_{p222}} P_{n+1}^{22\bullet} & P_n^{22\bullet} + M_3 \xrightarrow{k_{p223}} P_{n+1}^{23\bullet} \\
P_n^{21\bullet} + M_1 \underset{P_{21}k_{dp}}{\overset{k_{p211}}{\rightleftharpoons}} P_{n+1}^{11\bullet} & P_n^{21\bullet} + M_2 \xrightarrow{k_{p212}} P_{n+1}^{12\bullet} & P_n^{21\bullet} + M_3 \xrightarrow{k_{p213}} P_{n+1}^{13\bullet} \\
P_n^{23\bullet} + M_1 \xrightarrow{k_{p231}} P_{n+1}^{31\bullet} & P_n^{23\bullet} + M_2 \xrightarrow{k_{p232}} P_{n+1}^{32\bullet} & P_n^{23\bullet} + M_3 \xrightarrow{k_{p233}} P_{n+1}^{33\bullet} \\
P_n^{33\bullet} + M_1 \xrightarrow{k_{p331}} P_{n+1}^{31\bullet} & P_n^{33\bullet} + M_2 \xrightarrow{k_{p332}} P_{n+1}^{32\bullet} & P_n^{33\bullet} + M_3 \xrightarrow{k_{p333}} P_{n+1}^{33\bullet} \\
P_n^{31\bullet} + M_1 \underset{P_{31}k_{dp}}{\overset{k_{p311}}{\rightleftharpoons}} P_{n+1}^{11\bullet} & P_n^{31\bullet} + M_2 \xrightarrow{k_{p312}} P_{n+1}^{12\bullet} & P_n^{31\bullet} + M_3 \xrightarrow{k_{p313}} P_{n+1}^{13\bullet} \\
P_n^{32\bullet} + M_1 \xrightarrow{k_{p321}} P_{n+1}^{21\bullet} & P_n^{32\bullet} + M_2 \xrightarrow{k_{p322}} P_{n+1}^{22\bullet} & P_n^{32\bullet} + M_3 \xrightarrow{k_{p323}} P_{n+1}^{23\bullet}
\end{array}$$

Scheme 2. Terpolymerization chain growth with penultimate kinetics and depropagation.

$$\text{with} \quad Y = \frac{P_{33}k_{p_{332}}[M_2] + P_{13}k_{p_{132}}[M_2] + P_{23}k_{p_{232}}[M_2]}{P_{32}k_{p_{323}}[M_3] + P_{32}k_{p_{321}}[M_1] + P_{32}k_{p_{322}}[M_2]}, \quad \text{and}$$

$$\left(P_{22}k_{p_{221}}[M_1] + P_{32}k_{p_{321}}[M_1] + P_{12}k_{p_{121}}[M_1]\right) \bullet V - \left(P_{21}k_{p_{213}}[M_3] + P_{21}k_{p_{211}}[M_1] + P_{21}k_{p_{212}}[M_2] - P_{21}P_{11}k_{\text{dep}}\right) = 0 \quad (12)$$

$$\text{with} \quad V = \frac{P_{11}k_{p_{112}}[M_2] + P_{31}k_{p_{312}}[M_2] + P_{21}k_{p_{212}}[M_2]}{P_{12}k_{p_{123}}[M_3] + P_{12}k_{p_{121}}[M_1] + P_{12}k_{p_{122}}[M_2]}.$$

Equations 5, 7, and 9 can be rewritten in terms of radical molar fraction ($f_i = \frac{[P^{i\bullet}]}{\sum_{i=1}^{3}[P^{i\bullet}]}$):

$$Y \times f_3 - f_2 = 0 \quad (13)$$

$$V \times f_1 - f_2 = 0 \quad (14)$$

$$K \times f_1 - f_3 = 0 \quad (15)$$

$$\text{with} \quad K = \frac{P_{11}k_{p_{113}}[M_3] + P_{31}k_{p_{313}}[M_3] + P_{21}k_{213}[M_3]}{P_{13}k_{p_{133}}[M_3] + P_{13}k_{p131}[M_1] + P_{13}k_{p_{132}}[M_2]}, \quad \text{and}$$

$$f_1 + f_2 + f_3 = 1 \quad (16)$$

Equations 2–4, Eqs. 11–16, and the definitions of probabilities are solved simultaneously in PREDICI as a set of implicit equations.

The decomposition pathways of initiator TBPA in xylene at high temperatures are detailed elsewhere,[45,55,56] and the initiator efficiency f, representing the fraction of radicals successful in initiating polymerization, is set at 0.5 as in our previous work.[8,9,11,12,30,31] The value of f has only a small effect on predictions of residual monomer concentration for semibatch operation, but can influence MW predictions;[12] thus the value is coupled to the chain transfer to solvent constant, as discussed in previous work.[1] The termination coefficient k_t is assumed to be independent of conversion and weight-fraction polymer under these higher-temperature and low viscosity conditions, as in our previous articles.[1,2,8,9,11,12] The single rate coefficient ($k_{t,ter}$), however, varies with composition and is calculated according to a penultimate copolymerization model,[1,57,58] here extended to the three monomer system:

$$k_{t,ter}^{0.5} = (k_{t_{11}}^{0.5}P^{11\bullet} + k_{t_{12,12}}^{0.5}P^{12\bullet} + k_{t_{13,13}}^{0.5}P^{13\bullet} + k_{t_{22}}^{0.5}P^{22\bullet} + k_{t_{21,21}}^{0.5}P^{21\bullet} + k_{t_{23,23}}^{0.5}P^{23\bullet} + k_{t_{33}}^{0.5}P^{33\bullet} + k_{t_{31,31}}^{0.5}P^{31\bullet} + k_{t_{32,32}}^{0.5}P^{32\bullet})/(P^{1\bullet} + P^{2\bullet} + P^{3\bullet}) \quad (17)$$

The termination rate coefficients of BA secondary and midchain radicals were recently updated by Nikitin et al.[53] based on an extensive experimental data set, with a geometric mean used to estimate the rate coefficient for termination between a chain-end and midchain radical. Midchain radical termination is important for any acrylate-rich recipe, as the fraction of these radicals can become quite high due to their lower reactivity.[19,30,53] Chain transfer to monomer is not considered due to the low concentrations of free monomer relative to solvent and the dominance of other chain-transfer events in the system. The chain transfer rate coefficient of BA radicals to solvent (xylene) used in this work is slightly lower than that recently estimated by Nikitin et al.,[53] a difference attributable to the mixed xylene and ethylbenzene solvent used in that study.

As shown in Table 1, there are two kinds of midchain radicals, one formed by acrylate backbiting ($Q_{SCB}^{\bullet}$) and the other ($Q_{LCB}^{\bullet}$) by macromonomer propagation or long-chain branching mechanisms. As discussed in the Introduction, backbiting only occurs when BA is located in the pen-penultimate position and when BA is also the radical unit at the chain end. It is assumed that the rate of backbiting is reduced by a factor of 0.6 when ST or BMA is in the penultimate position, based upon our previous modeling of BA/ST copolymerization[31] and other literature.[32,33]

Long-chain branching is also assumed to occur only through intermolecular H-atom abstraction from a BA unit on the polymer chain. The rate coefficient for LCB in a BA homopolymerization is based on literature estimates summarized in a previous study,[30] with the ability of BMA and ST radicals to abstract H-atoms assumed proportional to their k_p values relative to BA. In a similar fashion, the addition rate of macromonomer to ST radical and BMA radical can be reasonably written as $0.55 \times k_{p222}/r_{21}$ and $0.55 \times k_{p111}$, as the macromonomer can be considered as a long-chain version of a methacrylate; k_{mac}/k_{p333} was previously estimated as 0.55 for BA homopolymerization at 138°C.[30] The midchain radicals formed by LCB or by macromonomer addition, $Q_{LCB}^{\bullet}$, can also undergo monomer addition and termination, with the same rate coefficients as for midchain radicals formed by backbiting. However, the β-scission of $Q_{LCB}^{\bullet}$ (as well as macromonomer addition to the midchain radicals) can be reasonably ignored, based on our previous study.[31]

The set of mechanisms in Table 1 is implemented in PREDICI, which automatically generates the reaction terms and species balances required to model the system, also taking into account the semibatch feeds. The simulations are run assuming isothermal conditions, as temperature control in the experimental system was excellent. Monomer, polymer, and solvent densities used in the model are as reported previously.[11,12,30]

Results and Discussion

ST/BMA/BA copolymerization and terpolymerization with varying composition

BMA/ST Copolymerization. BMA/ST semibatch experiments were run with monomer mass feed ratios of 100/0, 75/25, 25/75, and 0/100; the free monomer ([ST] and [BMA]) concentration profiles are plotted in Figure 1. The BMA/ST 50/50 system was detailed in Ref. 11 and is not shown here for the clarity of the figure. Table 3 lists the experimental and simulated final polymer weight-average M_w values. The unreacted ST and BMA monomer levels in the semibatch reactor, shown in Figure 1, are low throughout the course of these reactions, a characteristic of starved feed policy. Two sets of simulation results are shown, with (heavier lines) and without (lighter lines) methacrylate depropagation. The model including methacrylate depropagation provides good predictions for both [BMA] and [ST] levels, and M_w predictions are also reasonable. The model captures the observed increase in copolymer M_w with increasing ST content, but not the dip in M_w observed for the experiment with

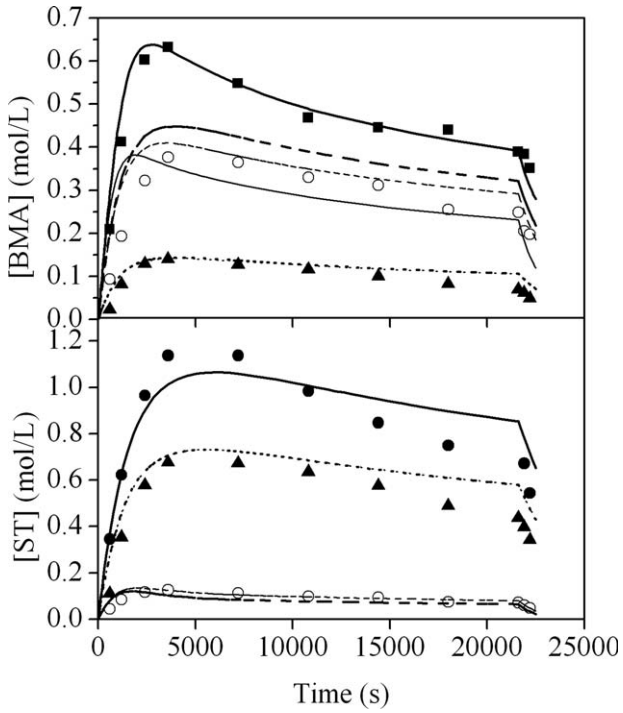

Figure 1. Monomer concentration ([BMA] and [ST]) experimental profiles (symbols) and model predictions (heavier lines for simulations with methacrylate depropagation, and lighter lines without) for ST/BMA semibatch copolymerizations at 138°C: BMA homopolymerization (■, —); BMA/ST 75/25 (○, - - -); BMA/ST 25/75 (▲, ···); ST homopolymerization (●, —).

Specified monomer mass ratios in the feed are for reactions with 70 wt % final polymer content and 2 wt % initiator relative to monomer.

75 wt % BMA in the feed relative to BMA homopolymerization. We have no explanation for this experimental finding, which was carefully checked. For all other conditions, simulation values are within 10% of experiment.

Without depropagation, simulated [BMA] levels are significantly lower than experimental for BMA homopolymerization. This mismatch decreases with the increasing fraction of ST in the system; the two simulation curves with and without methacrylate depropagation for ST/BMA 75/25 system are difficult to distinguish as they coincide almost exactly. As ST level in the copolymer increases, the probability of BMA diads at the growing chain end decreases significantly, especially because ST monomer prefers to be added to a methacrylate radical based on the monomer reactivity ratio ($r_{12} = 0.42$). Nonetheless, depropagation is an important mechanism to consider in methacrylate-rich recipes.

Table 3. Experimental and Simulated Final Polymer Weight-Average MW (M_w) Values for ST/BMA Semibatch Copolymerizations at 138°C

		Simulated M_w (g mol^{-1})	
BMA in the Feed (wt %)	Experimental M_w (g mol^{-1})	With Depropagation	Without Depropagation
100	14,630	13,590	14,220
75	11,440	15,074	15,385
50	15,461	16,130	16,190
25	16,530	16,930	16,940

ST/BA Copolymerization. Figure 2 shows free monomer ([BA] and [ST]) and polymer M_w profiles for ST/BA semibatch experiments with monomer mass feed ratios of 75/25 and 25/75. BA homopolymerization and BA/ST 50/50 systems were detailed in Refs. 30 and 31, and are not shown here for the clarity of the figure. Simulation results with (heavier lines) and without (lighter lines) acrylate backbiting are shown. (Simulations without backbiting also means that no chain scission and macromonomer reactions are included in the model, as both of these mechanisms arise from the formation of midchain radicals.) The separate effects of chain scission and macromonomer reactions on polymerization rate and M_w were detailed in our previous articles.[30,31]

Simulations with the full model, including backbiting, can represent the experimental monomer concentration and M_w profiles well. If these mechanisms are turned off so that no midchain radicals are formed, the faster polymerization rates

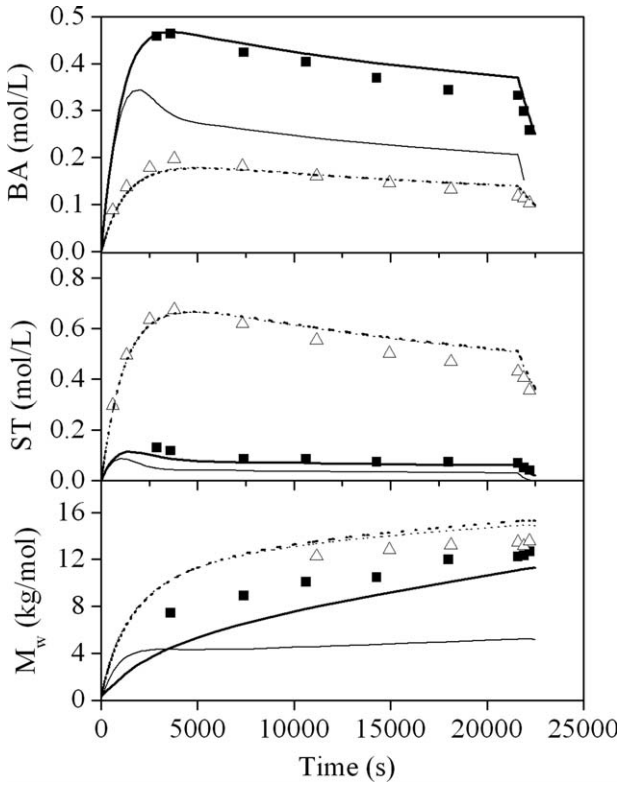

Figure 2. Monomer concentration ([BA] and [ST]), and weight-average molecular weight (M_w) experimental profiles (symbols) and model predictions (heavier lines for simulations with backbiting, and lighter lines without) for ST/BA semibatch copolymerizations at 138°C: ST/BA 75/25 (Δ, ···); ST/BA 25/75 (■, —).

Specified monomer mass ratios in the feed are for reactions with 70 wt% final polymer content and 2 wt% initiator relative to monomer.

Table 4. Experimental and Simulated Quarternary Carbon Levels (C_4%) of Polymers Produced via ST/BA 33/67 Semibatch Copolymerizations with Final Polymer Content 70 wt % at 140 and 160°C

Temperature (°C)	Experimental C_4%	Simulated C_4%	
		$k_{bb'}/k_{bb} = 0.6$	$k_{bb'}/k_{bb} = 1.0$
140	3.34	4.03	8.54
160	5.68	5.98	9.89

Simulated values compare the effect of reducing the backbiting rate coefficient when styrene is in the penultimate position ($k_{bb'}/k_{bb} = 0.6$) to simulations performed with no reduction in the rate coefficient ($k_{bb'}/k_{bb} = 1.0$).

of secondary radicals lead to very low predicted free monomer levels for the system with high BA level (75%) in the recipe. The M_w level as well as the significant increase observed over time also cannot be matched by the simpler model, as no secondary acrylate reactions, including chain scission and macromonomer incorporation, are available.[31] The importance of these reactions decreases with the increasing fraction of ST in the recipe; the two simulation cases for the BA/ST 25/75 recipe almost overlap, both in free monomer and M_w predictions. These simulations demonstrate that the backbiting/scission/macromer side reactions are important for any recipe with high acrylate content.

As discussed previously, the acrylate backbiting rate with ST in the penultimate position was reduced by a factor of 0.6 compared with the BA homopolymerization case.[31] Table 4 quantifies the effect of this adjustment by comparing model predictions to experimental values of the level of quaternary carbons found in the final polymers (C_4%), a structure that results from acrylate backbiting (see Scheme 1). The results shown are for copolymers produced with a ST/BA 33/67 recipe and final polymer content of 70 wt % at 140 and 160°C. k_{bb} represents the backbiting rate of BA radicals with BA as adjacent unit, and $k_{bb'}$ is the backbiting rate of BA radicals with ST as adjacent unit. As shown in Table 4, the experimental C_4% value increases with increased temperature, due to the higher activation energy for backbiting compared with chain growth. (The combined effect of β-scission and macromer addition reactions on C_4% is very small.[30]) The experimental results are represented well by the model that assumes ST reduces the rate coefficient for backbiting, whereas simulated C_4% values are too high by a factor of 2 without this adjustment. This subtle effect can only be observed by examining the resultant polymer structure by ^{13}C NMR, as the small adjustment in $k_{bb'}$ has no observable impact on free monomer or MW profiles.

BMA/ST/BA Terpolymerization. The copolymerization results presented were chosen to show the importance of acrylate and methacrylate side reactions on these high-temperature starved-feed reaction systems. These reactions have been included in the full terpolymerization model, as well as penultimate propagation and termination kinetics. Figure 3 shows the monomer ([BMA], [ST], and [BA]) concentration and M_w profiles for BMA/ST/BA semibatch experiments at 138°C with monomer mass feed ratios of 70/15/15, 50/25/25, 33/33/33, and 15/15/70. Note that all of the rate coefficients used in the terpolymerization model were taken from our previous copolymerization work and literature. The excellent agreement between model and experimental

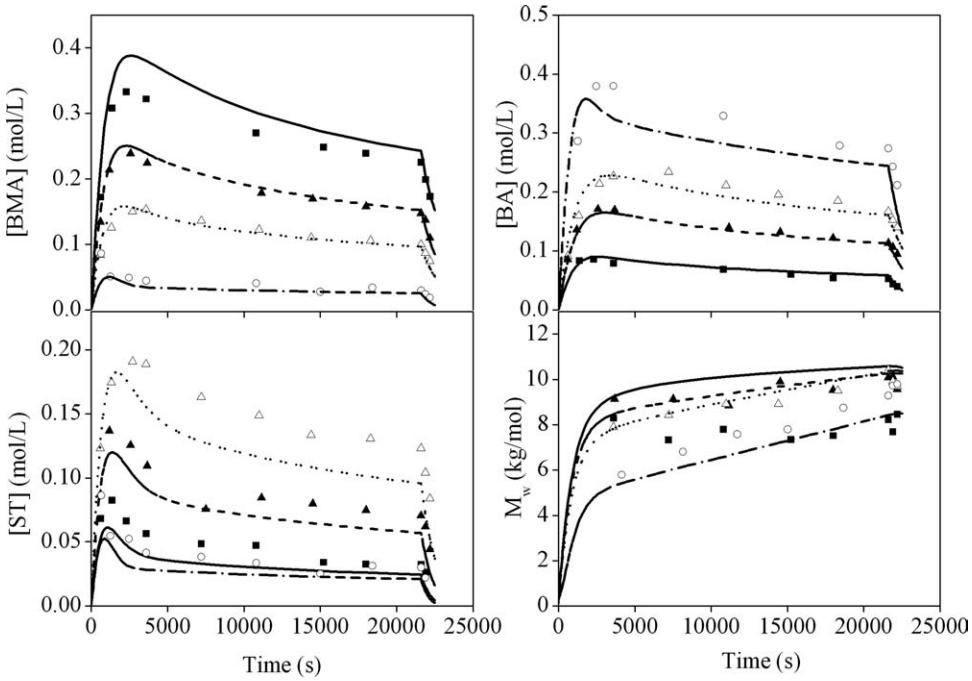

Figure 3. Monomer concentration ([BMA], [BA], and [ST]) and weight-average molecular weight (M_w) experimental profiles (symbols) and model predictions (lines) for BMA/ST/BA semibatch terpolymerizations at 138°C: BMA/ST/BA 70/15/15 (■, —); BMA/ST/BA 50/25/25 (▲, - - -); BMA/ST/BA 33/33/33 (Δ, ···); BMA/ST/BA 15/15/70 (○, -·-).

Specified monomer mass ratios in the feed are for reactions with 70 wt % final polymer content, monomer feeding time 6 h, and 2 wt % initiator relative to monomer.

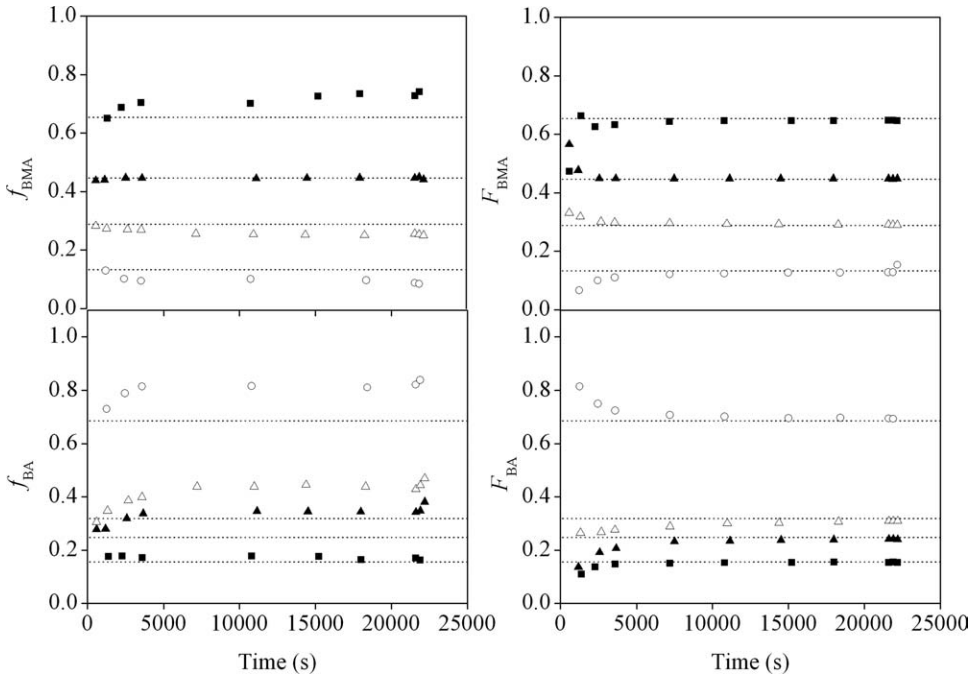

Figure 4. Monomer fraction (left two plots; f_{BMA} and f_{BA}) and cumulative terpolymer composition (right two plots; F_{BMA} and F_{BA}) in the semibatch reactions, as determined from GC measurement of residual monomer and calculated by mass balance for the feed ratios (wt %): BMA/ST/BA 70/15/15 (■); BMA/ST/BA 50/25/25 (▲); BMA/ST/BA 33/33/33 (△); BMA/ST/BA 15/15/70 (○).

Horizontal lines indicate the monomer feed ratio converted to a molar basis.

profiles is an indication that we have achieved a good understanding of this complex terpolymerization system. The one exception is the M_w prediction for the 70/15/15 recipe with high BMA content; as observed for the BMA/ST copolymer system, the model consistently overpredicts MW by 20–30% for this condition.

As a characteristic of starved feed policy, the monomer and polymer compositions of BMA and BA (and thus also ST) remain constant throughout the reactions (Figure 4). The terpolymer compositions are well-controlled by the monomer feed ratios as seen by the perfect match of the composition data. At low BMA feed compositions, BMA is preferentially incorporated into the terpolymer, as governed by the reactivity ratios. The free monomer fraction of BA in the reactor is always higher than that in the feed composition for all experiments. In all cases, the relative amounts of monomer in the system naturally adjust to a steady-state level (well-predicted by the model, see Figure 3) that keeps the terpolymer composition on target, an inherent feature of semibatch starved-feed operation.

The necessity of considering penultimate chain-growth kinetics (see Scheme 2) for the terpolymerization system was verified by a pulsed-laser polymerization study.[50] It is also useful to consider the impact of these mechanisms on semibatch operation. For the 33/33/33 experiment shown in Figure 3, experimental monomer concentrations ([BMA] = 0.099, [ST] = 0.123, [BA] = 0.167, all values in mol l^{-1}) at the end of the 6 h monomer feed are well-predicted by the full model ([BMA] = 0.096, [ST] = 0.090, [BA] = 0.150). If penultimate chain-growth kinetics are not considered ($s_1 = s_2 = s_3 = 1.0$), reaction rate increases such that the predicted monomer concentrations are low by more than 25% ([BMA] = 0.069, [ST] = 0.063, [BA] = 0.109). More importantly, the predicted M_w value without considering penultimate effects is significantly higher at 13.4 kg mol^{-1} compared with the experimental value of 9.7 kg mol^{-1}, which is well-matched by the full model prediction of 9.9 kg mol^{-1}. Clearly, penultimate effects in this acrylic terpolymerization system must be accounted for.

BMA/ST/BA 33/33/33 with Varying Final Polymer Levels. The ability to predict polymer MWs for recipes run with differing final polymer content is a major requirement for a generalized model. We have shown that our ST/methacrylate model can capture the observed change in M_w values found experimentally.[1] Here, the full model will be tested by comparing with BMA/ST/BA 33/33/33 terpolymerization experiments conducted with different final polymer contents. Figure 5 shows polymer weight- and number-average M_w and M_n values and polymer content for BMA/ST/BA 33/33/33 semibatch terpolymerizations conducted at 140°C and a monomer feeding time of 3 h with two different final polymer levels (70 wt % and 30 wt %). The faster monomer feed rate (corresponding to higher final polymer content) leads to significantly higher polymer M_w, as shown in Figure 5. The model successfully captures this effect as well as the polydispersity (M_n and M_w profiles) of the resultant polymer.

In addition, the effect of monomer feeding time on M_w can be seen by comparing the 33/33/33 BMA/ST/BA MW profiles in Figure 3 (6 h feed time) and Figure 5 (3 h feed time). The final M_w value with the shorter feed time (Figure

5) is almost twice that obtained with the 6 h feed time (Figure 3). This difference, well-captured by the model, is related to the higher free monomer levels that occur when monomer feed time is shortened. Monomer levels are also the principal factor why higher final polymer content lead to higher M_w values for identical feed times.

BMA/ST/BA 33/33/33 with varying reaction temperature

The generality of the model is also demonstrated by comparing to experimental data obtained at different reaction temperatures. Figure 6 shows polymer M_w and M_n values and polymer content for BMA/ST/BA 33/33/33 semibatch terpolymerizations conducted at 140 and 160°C with a final polymer content of 70 wt % and monomer feed time of 3 h. Lower polymer MWs are obtained at the higher reaction temperature. Depropagation[9] and acrylate side reactions[30,53] increase in importance with increasing temperature. However, in this case, the decrease in M_w can be primarily attributed to transfer to solvent instead of any secondary reactions, as the effects of depropagation and acrylate backbiting are significantly suppressed with the 33/33/33 recipe. The simulated final M_w values calculated without including transfer to solvent are 26 kg mol^{-1} at 140°C and 30 kg mol^{-1} at 160°C, much higher than the experimental values shown in Figure 6.

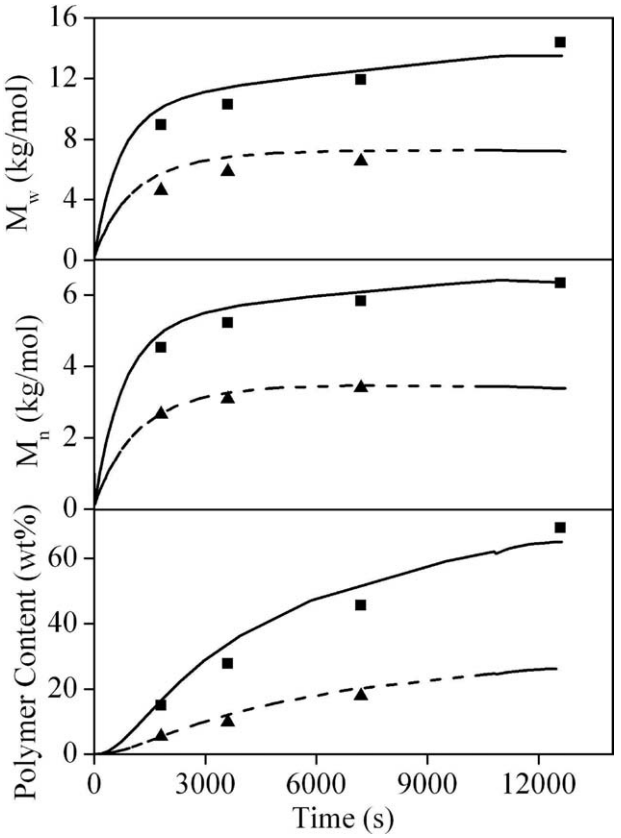

Figure 5. Weight- and number-average molecular weight (M_w and M_n) and polymer content (wt %) experimental profiles (■, 70 wt % final polymer content; ▲, 30 wt %) and model predictions (solid line, 70 wt %; dashed line, 30 wt %) for BMA/ST/BA 33/33/33 semibatch terpolymerizations at 140°C and monomer feed time of 3 h with different final polymer contents.

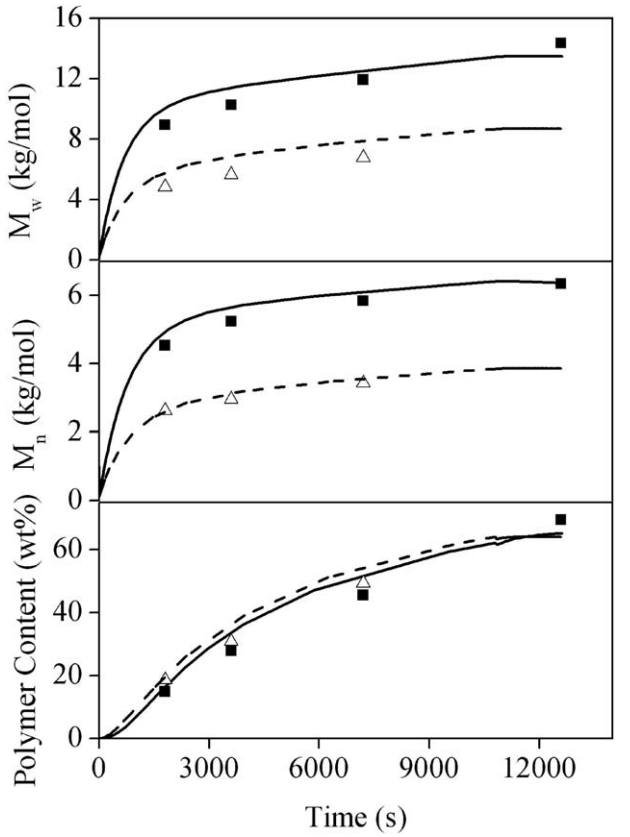

Figure 6. Weight- and number-average molecular weight (M_w and M_n) and polymer content (wt %) experimental profiles (■, 140°C; Δ, 160°C) and model predictions (solid lines, 140°C; dashed lines, 160°C) for BMA/ST/BA 33/33/33 semibatch terpolymerizations at different temperatures with 70% final polymer content and 1.5 mol % initiator relative to monomer.

Conclusions

n-Butyl methacrylate/styrene/*n*-butyl acrylate (BMA/ST/BA) high-temperature starved-feed solution semibatch copolymerization and terpolymerization experiments with varying monomer feed compositions, final polymer contents, monomer feed times, and reaction temperatures were carried out. A generalized comprehensive mechanistic terpolymerization model of the system implemented in PREDICI includes methacrylate depropagation, acrylate backbiting, chain scission, and macromonomer propagation, as well as considers the effect of penultimate units on propagation and termination kinetics. The impact of these secondary reactions on monomer concentration and MW was shown to be quite dependent on polymer composition: methacrylate depropagation has a large effect on results for recipes containing significant methacrylate fractions, and the backbiting/scission/

macromer side reactions are of considerable importance if the acrylate content is high. The backbiting rate coefficient is slightly affected by the identity of the penultimate unit on the chain, as shown by ^{13}C NMR measure of quarternary carbons in the polymer chain. However, it is necessary to include all of these reactions to completely cover the range of temperatures and compositions typically used to produce acrylic resins. The generality of the terpolymerization mechanistic model was verified against data obtained under a range of polymerization conditions at two laboratories and provides an exclusive insight into the kinetic complexity of methacrylate/ST/acrylate terpolymerization at high temperatures. Although mainly tested against semibatch operation conditions, the mechanistic set can be used to represent any solution styrene/methacrylate/acrylate terpolymerization system at elevated temperatures that does not exhibit a strong gel effect.

Acknowledgments

We thank E. I. du Pont de Nemours and Co. and the Natural Sciences and Engineering Research Council of Canada for financial support of this work. We also thank John Richards for helpful discussions regarding model implementation, and Domenic Barsotti, Christopher Bruni, George Kalfas, and Thomas Scholz for providing MW (Figures 5 and 6) and ^{13}C NMR (Table 4) results from experiments conducted at the DuPont Marshall Laboratory.

Literature Cited

1. Wang W, Hutchinson RA. Recent advances in the study of high-temperature free radical acrylic solution copolymerization. *Macromol React Eng*. 2008;2:199–214.
2. Grady MC, Simosick WJ, Hutchinson RA. Studies of higher temperature polymerization of n-butyl methacrylate and n-butyl acrylate. *Macromol Symp*. 2002;182:149–168.
3. Adamsons K, Blackman G, Gregorovick B, Lin L, Matheson R. Oligomers in the evolution of automotive clearcoats: mechanical performance testing as a function of exposure. *Prog Org Coat*. 1998;34:64–74.
4. Buder-Stroisznigg M, Wallner GM, Straub B, Jandel L, Lang RW. Structure-property correlations of flexible clear coats. *Prog Org Coat*. 2009;65:328–332.
5. Bywater S. Photosensitized polymerization of methyl methacrylate in dilute solution above 100 °C. *Trans Faraday Soc*. 1955;51:1267–1273.
6. Hutchinson RA, Paquet DA Jr., Beuermann S, McMinn JH. Investigation of methacrylate free-radical depropagation kinetics by pulsed-laser polymerization. *Ind Eng Chem Res*. 1998;37: 3567–3574.
7. O'Driscoll KF, Burczyk AF. Kinetics of styrene and methyl methacrylate polymerizations in a starved feed reactor. *Polym React Eng*. 1992;1:111–144.
8. Li D, Grady MC, Hutchinson RA. High-temperature semibatch free radical copolymerization of butyl methacrylate and butyl acrylate. *Ind Eng Chem Res*. 2005;44:2506–2517.
9. Wang W, Hutchinson RA, Grady MC. Study of butyl methacrylate depropagation behavior using batch experiments in combination with modeling. *Ind Eng Chem Res*. 2009;48:4810–4816.
10. Ivin KJ. Thermodynamics of addition polymerization. *J Polym Sci A: Polym Chem*. 2000;38:2137–2146.
11. Li D, Hutchinson RA. High temperature semibatch free radical copolymerization of butyl methacrylate and styrene. *Macromol Symp*. 2006;243:24–34.
12. Wang W, Hutchinson RA. High temperature semibatch free radical copolymerization of dodecyl methacrylate and styrene. *Macromol Symp*. 2008;261:64–73.
13. Lowry GG. Effect of depropagation on copolymer composition. I. General theory for one depropagating monomer. *J Polym Sci*. 1960;42:463–477.
14. Li D, Li N, Hutchinson RA. High-temperature free radical copolymerization of styrene and butyl methacrylate with depropagation and penultimate kinetic effects. *Macromolecules*. 2006;39: 4366–4373.
15. Li D, Leiza JR, Hutchinson RA. High temperature free radical copolymerization with depropagation and penultimate kinetic effects. *Macromol Theory Simul*. 2005;14:554–559.
16. Ahmad NM, Heatley F, Lovell PA. Chain transfer to polymer in free-radical solution polymerization of n-butyl acrylate studied by NMR spectroscopy. *Macromolecules*. 1998;31:2822–2827.
17. Plessis C, Arzamendi G, Leiza JR, Schoonbrood AS, Charmot D, Asua JM. A decrease in effective acrylate propagation rate constants caused by intramolecular chain transfer. *Macromolecules*. 2000;33:4–7.
18. Yamada B, Azukizawa M, Yamazoe H, Hill D, Pomery P. Free radical polymerization of cyclohexyl acrylate involving interconversion between propagating and mid-chain radicals. *Polymer*. 2000;41: 5611–5618.
19. Nikitin AN, Hutchinson RA. The effect of intramolecular transfer to polymer on stationary free radical polymerization of alkyl acrylates. *Macromolecules*. 2005;38:1581–1590.
20. Chiefari J, Jeffery J, Mayadunne RTA, Moad G, Rizzardo E, Thang SH. Chain transfer to polymer: a convenient route to macromonomers. *Macromolecules*. 1999;32:7700–7702.
21. Hirano T, Yamada B. Stereospecificity in radical polymerization of methyl α-(chloromethyl)acrylate. *Polymer*. 2003;44:4481–4486.
22. Peck ANF, Hutchinson RA. Secondary reactions in the high-temperature free radical polymerization of butyl acrylate. *Macromolecules*. 2004;37:5944–5951.
23. Busch M, Müller M. Simulating acrylate polymerization reactions: toward improved mechanistic understanding and reliable parameter estimates. *Macromol Symp*. 2004;206:399–418.
24. Quan C, Soroush M, Grady MC, Hansen JE. High-temperature homopolymerization of ethyl acrylate and n-butyl acrylate: polymer characterization. *Macromolecules*. 2005;38:7619–7628.
25. Rantow FS, Soroush M, Grady MC, Kalfas GA. Spontaneous polymerization and chain microstructure evolution in high-temperature solution polymerization of n-butyl acrylate. *Polymer*. 2006;47:1423–1435.
26. Junkers T, Koo SPS, Davis TP, Stenzel MH, Barner-Kowollik C. Mapping poly(butyl acrylate) product distributions by mass spectrometry in a wide temperature range: suppression of midchain radical side reactions. *Macromolecules*. 2007;40:8906–8912.
27. Junkers T, Barner-Kowollik C. The role of mid-chain radicals in acrylate free radical polymerization: branching and scission. *J Polym Sci Part A: Polym Chem*. 2008;46:7585–7605.
28. Yamada B, Oku F, Harada T. Substituted propenyl end groups as reactive intermediates in radical polymerization. *J Polym Sci Part A: Polym Chem*. 2003;41:645–654.
29. Harada T, Zetterlund PB, Yamada B. Preparation of macromonomers by copolymerization of methyl acrylate dimer involving β-fragmentation. *J Polym Sci Part A: Polym Chem*. 2004;42:597–607.
30. Wang W, Nikitin AN, Hutchinson RA. Consideration of macromonomer reactions in butyl acrylate free radical polymerization. *Macromol Rapid Commun*. 2009;30:2022–2027.
31. Wang W, Hutchinson RA. High temperature semibatch free radical copolymerization of styrene and butyl acrylate. *Macromol Symp*. 2010;289:33–42.
32. Plessis C, Arzamendi G, Leiza JR, Schoonbrood HAS, Charmot D, Asua JM. Kinetics and polymer microstructure of the seeded semibatch emulsion copolymerization of n-butyl acrylate and styrene. *Macromolecules*. 2001;34:5147–5157.
33. González I, Asua JM, Leiza JR. The role of methyl methacrylate on branching and gel formation in the emulsion copolymerization of BA/MMA. *Polymer*. 2007;48:2542–2547.
34. Gao J, Penlidis A. A comprehensive simulator/database package for bulk/solution free-radical terpolymerizations. *Macromol Chem Phys*. 2000;201:1176–1184.
35. Dubé MA, Soares JBP, Penlidis A, Hamielec AE. Mathematical modeling of multicomponent chain-growth polymerizations in batch,

semibatch, and continuous reactors: a review. *Ind Eng Chem Res*. 1997;36:966–1015.
36. Keramopoulos A, Kiparissides C. Mathematical modeling of diffusion-controlled free-radical terpolymerization reactions. *J Appl Polym Sci*. 2003;88:161–176.
37. McManus NT, Hsieh G, Penlidis A. Free radical terpolymerization of butyl acrylate/methyl methacrylate and alpha methyl styrene at high temperature. *Polymer*. 2004;45:5837–5845.
38. Leamen MJ, McManus NT, Penlidis A. Terpolymerization with depropagation: modelling the copolymerization of the methyl methacrylate/alpha-methylstyrene/butyl acrylate system. *Chem Eng Sci*. 2006;61:7774–7785.
39. Wulkow M. Computer aided modeling of polymer reaction engineering-the status of Predici, 1 – simulation. *Macromol React Eng*. 2008;2:461–494.
40. Wang W, Hutchinson RA. PLP/SEC/NMR study of free radical copolymerization of styrene and glycidyl methacrylate. *Macromolecules*. 2008;41:9011–9018.
41. Penzel E, Götz N. Solution properties of polyacrylic esters. I. Light scattering and viscosity measurements in tetrahydrofuran. *Angew Makromol Chem*. 1990;178:191–200.
42. Hutchinson RA, McMinn JH, Paquet DA Jr., Beuermann S, Jackson C. A pulsed-laser study of penultimate copolymerization propagation kinetics for methyl methacrylate/n-butyl acrylate. *Ind Eng Chem Res*. 1997;36:1103–1113.
43. Seferis JC. *Refractive indices of polymers*. In: Brandrup J, Immergut EH, Grulke EA, editors. *Polymer Handbook*, 4th ed. New York: Wiley, 1999.
44. Li D. *Modeling of Kinetic Complexities in High Temperature Free Radical Polymerization for Production of Acrylic Coatings Resins*. PhD Thesis, Kingston, ON: Queen's University, 2006.
45. Buback M, Klingbeil S, Sandmann J, Sderra MB, Vögele HP, Wackerbarth H, Wittkowski L. Pressure and temperature dependence of the decomposition rate of tert-butyl peroxyacetate and of tert-butyl peroxypivalate. *Z Phys Chem (Muenchen, Ger.)*. 1999;210:199–221.
46. Beuermann S, Buback M, Davis TP, Gilbert RG, Hutchinson RA, Kajiwara A, Klumpermann B, Russell GT. Critically evaluated rate coefficients for free-radical polymerization, 3a: propagation rate coefficients for alkyl methacrylates. *Macromol Chem Phys*. 2000;201:1355–1364.
47. Buback M, Gilbert RG, Hutchinson RA, Klumpermann B, Kuchta F, Manders BG, O'Driscoll KF, Russell GT, Schweer J. Critically evaluated rate coefficients for free-radical polymerization. 1. Propagation rate coefficient for styrene. *Macromol Chem Phys*. 1995;196:3267–3280.
48. Asua JM, Beuermann S, Buback M, Castignolles P, Charleus B, Gilbert RG, Hutchinson RA, Leiza JR, Nikitin AN, Vairon JP, van Herk AM. Critically evaluated rate coefficients for free-radical polymerization. 5. Propagation rate coefficient for butyl acrylate. *Macromol Chem Phys*. 2004;205:2151–2160.
49. Hakim M, Verhoeven V, Mcmanus NT, Dubé MA, Penlidis A. High-temperature solution polymerization of butyl acrylate/methyl methacrylate: reactivity ratio estimation. *J Appl Polym Sci*. 2000;77:602–609.
50. Li D, Hutchinson RA. Penultimate propagation kinetics of butyl methacrylate, butyl acrylate, and styrene terpolymerization. *Macromol Rapid Commun*. 2007;28:1213–1218.
51. Barth J, Buback M, Hesse P, Sergeeva T. Chain-length-dependent termination in n-butyl methacrylate and tert-butyl methacrylate bulk homopolymerizations studied via SP-PLP-ESR. *Macromolecules*. 2009;42:481–488.
52. Beuermann, S, Buback M. Rate coefficients of free-radical polymerization deduced from pulsed laser experiments. *Prog Polym Sci*. 2002;27:191–254.
53. Nikitin AN, Hutchinson RA, Wang W, Kalfas GA, Richards JR, Bruni C. Effect of intramolecular transfer to polymer on stationary free radical polymerization of alkyl acrylates, 5-consideration of solution polymerization up to high temperatures. *Macromol React Eng*. In press 2010.
54. Nikitin AN, Hutchinson RA, Kalfas GA, Richards JR, Bruni C. The effect of intramolecular transfer to polymer on stationary free-radical polymerization of alkyl acrylates, 3—consideration of solution polymerization up to high conversions. *Macromol Theory Simul*. 2009;18:247–258.
55. Wang W, Hutchinson RA. Evidence of scission products from peroxide-initiated higher temperature polymerization of alkyl methacrylates. *Macromolecules*. 2009;42:4910–4913.
56. Buback M, Sandmann J. Pressure and temperature dependence of the decomposition rate of aliphatic tert-butyl peroxyesters. *Z Phys Chem (Muenchen, Ger)*. 2000;214:583–607.
57. Buback M, Kowollik C. Termination kinetics in free-radical bulk copolymerization: the systems dodecyl acrylate-dodecyl methacrylate and dodecyl acrylate-methyl acrylate. *Macromolecules*. 1999;32:1445–1452.
58. Buback M, Feldermann A. Termination kinetics of free-radical methyl methacrylate-dodecyl acrylate and dodecyl methacrylate-methyl acrylate copolymerizations. *Aust J Chem*. 2002;55:475–481.

Manuscript received Oct. 29, 2009, and revision received Mar. 9, 2010.